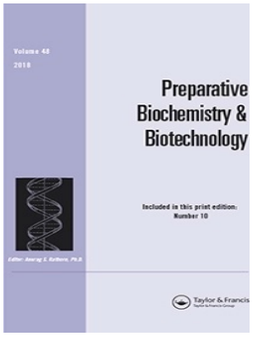

Preparative Biochemistry and Biotechnology

ISSN: 1082-6068 (Print) 1532-2297 (Online) Journal homepage: https://www.tandfonline.com/loi/lpbb20

A new biosensor for osteoporosis detection

Sevilay Inal Kabala, Hulya Yagar & Hakkı Mevlut Ozcan

To cite this article: Sevilay Inal Kabala, Hulya Yagar & Hakkı Mevlut Ozcan (2019): A new biosensor for osteoporosis detection, Preparative Biochemistry and Biotechnology, DOI: 10.1080/10826068.2019.1587628

To link to this article: https://doi.org/10.1080/10826068.2019.1587628

Published online: 19 Mar 2019.

PREPARATIVE BIOCHEMISTRY AND BIOTECHNOLOGY
https://doi.org/10.1080/10826068.2019.1587628

A new biosensor for osteoporosis detection

Sevilay Inal Kabala[a], Hulya Yagar[b], and Hakkı Mevlut Ozcan[b]

[a]Health Services Vocational High School, Kırklareli University, Kırklareli, Turkey; [b]Department of Chemistry, Faculty of Science, Trakya University, Edirne, Turkey

ABSTRACT

Osteoporosis is a disease that is characterized by deterioration of bone tissue and increased risk of fracture as it leads to a decrease in bone mineral density, which is an important public health problem. Today, bone mineral density is measured by radiological techniques. Alternative techniques are needed because of the disadvantages such as excessive radiation intake, the cost of radiological techniques, and the necessity for specialist personnel for the devices. The quantitative determination of biochemical markers that play a role in bone mineralization may be a good alternative for the osteoporosis diagnosis and especially in the follow-up of treatment.

In this study, a specific and sensitive immunological biosensor, which quantitatively determines the osteocalcin molecule, has been developed to be used in the early osteoporosis diagnosis and to evaluate the response to the drug treatment. Anti-osteocalcin antibody was immobilized onto gold electrode surface via covalent immobilization method by using 6-mercaptohexanol, 1,4-butanedioldiglycidyl ether, ethanolamine, and glutaraldehyde. Immobilization steps and biosensor characterization were specified by cyclic voltammetry and electrochemical impedance spectroscopy. The detection time and range of Ocn biosensor were determined as 45 min and 10–60 pg μL^{-1} Ocn concentration, respectively. The Ocn biosensor was successfully applied in artificial serum samples spiked with Ocn.

KEYWORDS

Osteocalcin; osteoporosis; biosensor; electrochemical impedance spectroscopy; 1,4-butanedioldiglycidyl ether; self-assembled monolayer

Introduction

Osteoporosis is a bone disease characterized by low bone mass, deterioration in microstructure, and consequently an increase in the likelihood of fracture.[1–3] Approximately, 200 million people worldwide are thought to be suffering from osteoporosis.[4] In the world, one out of every three women and one out of five men over 50 years of age have osteoporotic fractures.[5] Especially women who are in the post-menopausal period and old men are in risky groups.

Bone mineral density (BMD) measurement and Dual-Energy-X-ray (DEXA) are commonly used in the diagnosis of osteoporosis.[6] However, these techniques have some limitations. The costs of technologies and the monitoring of bone loss require at least 2–3 years. This reveals the importance and the necessity for instantaneous measurement of bone metabolism.[7] The state of the bone cycle is monitored by measuring the biochemical markers. ELISA, RIA, and HPLC are the most widely used methods to detect biochemical markers of bone turnover.[8] Despite high accuracy, these techniques are both costly and require large bulky devices. Also, they are time-consuming and technically trained personnel are needed. Recently, the advances in biosensor technology may allow the evaluation of the metabolic status of the bone. Since biosensors are the measurement systems, which can easily analyze the compounds with a lower cost when compared to other methods, low-cost, fast, reliable, and high-precision biosensors may be developed to use in the osteoporosis diagnosis.

The biochemical markers of bone turnover may reflect the state of bone metabolism in real time and show bone status in real time. They may provide information about the risk of osteoporotic fracture and response to treatment.[9] They cannot provide a diagnosis alone, but they are very useful in the post-treatment and respond more quickly to BMD in evaluating the response after treatment. During the mineralization and resorption of the bone cycle, a number of bone matrix elements pass into the blood and urine. These elements are biochemical markers of bone and are divided to two categories: Bone-building markers and bone destruction markers. Bone building markers are Ocn, bone-specific alkaline phosphatase (BALP), procollagen Type 1 N-Terminal (P1NP),[10] and procollagen Type 1 C-Terminal (P1CP). Bone destruction markers are bone sialoprotein (BSP), C-terminal tip telopeptide of type 1 collagen (CTx),[10] N-terminal telopeptide of type 1 collagen (NTx), hydroxy pyrrole, hydroxylysine, deoxypyridinoline (DPD), pyridinium crosslinks (crosslinks), and tartrate-resistant acid phosphatase (TRAP). Since these biochemical markers are the most commonly used biomolecules to evaluate bone turnover, the biosensors designed for the bone biomarkers can be used to monitor the osteoporosis treatment process and to evaluate drug efficacy.[11,12]

CONTACT Sevilay Inal Kabala inal.sevilay@gmail.com, sevilay.inal@klu.edu.tr Health Services Vocational High School, Kırklareli University, Kavaklı Campus, Kırklareli, Turkey.

Ocn is the most abundant non-collagenous protein in the bone structure.[13] It is a protein with 44-amino acid (5.8 kDa) length which is synthesized by osteoblasts.[14] Most of the Ocn molecules bind the inorganic part of the bone (hydroxyapatite) into the bone matrix. Vitamin K-dependent asit-glutamyl carboxy transferase converts glutamic acid residues (Glu) at positions 17, 21, and 24 of the Ocn molecule into the gamma-glutamic acids.[15] This modification increases the negative charge density of Ocn molecule, thus provides to have high affinity to calcium and hydroxyapatite and become more stabilized the α-helical structures, and also Ocn plays a role in bone calcification by binding calcium ions. Because it is released from the matrix to circulation during bone resorption, it is considered to be a sign of bone turnover.[16] Also, it increases vitamin D synthesis.[17] The serum Ocn levels increase in some diseases including paget disease, acromegaly, puberty, primary hyperparathyroidism, hyperthyroidism, renal osteodystrophy and untreated osteomalacia, metastatic bone diseases, whereas they decrease in some patients treated with glucocorticoid such as hypoparathyroidism, hypothyroidism, Cushing's syndrome, multiple myeloma, and malignant hypercalcemia in estrogen use.[18] Recently, it has been suggested that there may be a relationship between Ocn, obesity, and insulin resistance.[19,20] Ocn is a specific and sensitive marker to evaluate the risk of osteoporosis and to monitor treatment responses.[21] Ocn level is generally considered to be 9–42 μg L^{-1} in individuals over 18 years of age. Clinically, Ocn amount in serum is determined by using ELISA (Enzyme-Linked Immunosorbent Assay) and RIA method.

In this study, we developed an Ocn biosensor based on Electrochemical Impedance Spectroscopy (EIS) to use in Ocn analysis of samples. EIS is widely used in electrochemical measurements of molecular interactions and various biosensor applications. Traditional applications of EIS include immuno-sensor protocols that use immobilized antibodies to determine protein-protein interactions[22] or detect smaller molecules such as antibiotics[23] in complex biological environments. Impedance spectroscopy is a powerful method for analyzing the complex electrical resistance of a system and is sensitive to changes in the surface. It is particularly suitable for detecting binding events on the surface of the physical component. Thus, in addition to the detection of biological recognition processes, it is used as a valuable tool for characterizing surface modifications that occur during the immobilization of biomolecules on the physical component. EIS is a selective and label-free method to determine a variety of analytes, especially biomarkers.[24] Moreover, EIS is an electroanalytical measurement technique that does not impair the very small integrity of the applied surfaces. It provides much more information compared to measurement techniques based on capacitance or conductivity.

In electroanalysis, the gold electrode is highly preferred as the physical component. The main reason for the popularity of gold is that it is not only inert but also biocompatible. For example, by utilizing different thiol-based immobilization chemicals, molecules can be crosslinked on gold electrode surface.[25] Self-assembled monolayers (SAM) are often used to immobilization of the desired element to the support material. Long chain thiols can effectively secure the electrode surface from unwanted reactions and therefore are often used in capacitive sensors. Disulfides, sulfides, and thiols are strongly coordinated on various metals (gold, silver, platinum, or copper).

In this study, an electrochemical biosensor system was developed for the precise, sensitive and practical determination of Ocn concentration by using a SAM strategy. The presented biosensor is label-free immunosensor, and first impidimetric biosensor in literature used for Ocn determination. Also, 1,4-BDE (1,4-butanediol diglycidyl ether) which is a well-acknowledged as cross linker was used first time in a biosensor design. In the fabrication of Ocn biosensor, SAM on Au electrode surface was generated using 6-mercaptohexanol (6-MCH). After 1,4-BDE (1,4-butanediol diglycyl ether) was covalently attached to SAM, the construction of the biosensor was completed with Anti-Ocn immobilization by means of ethanolamine (EA) and glutaraldehyde (GLT) as cross-linker.

Experimental

Materials and methods

All reagents (Ocn, Anti-Ocn, 1,4-Butanediol diglycyl ether, Ethanolamine, Glutaraldehyde, and artificial serum) were purchased from Sigma-Aldrich. The biomolecules of Ocn and Anti-Ocn were prepared at certain concentrations and stored at −20 °C (Ocn) and −80 °C (Anti-Ocn) until used. A three electrode system consisting of working gold electrode (2.01 mm^2 surface area), Ag/AgCl reference electrode (used saturated KCl solution as electrolyte), and a Platinum counter electrode was housed in a 15 mL electrochemical cell. These three electrodes were provided from BASi, Warwickshire, UK. All electrochemical experiments were carried out using a Gamry Interface 1000 Potentiostat/Galvanostat (Gamry Instruments, Warminster, USA) interfaced with a PC via an ECM Analyst software (Gamry Instruments, Warminster, USA).

SAM modification of gold electrodes with 6-MCH

The working electrode (Au electrode) was cleaned with both mechanical and chemical cleaning procedures to remove the impurities attached to the surface. The cleaning procedure was repeated before each biosensor fabrication. With the help of a spatula, a small amount of aluminum oxide was put on the surface cleaning pad and mixed with a few drops of ultrapure water until viscous consistency is achieved. The electrode surface was mechanically cleaned with this paste during 1 min. After washing the electrode with ultrapure water, it was sonicated in absolute ethanol (99.9%) in order to remove the particles attached to the surface. It was rinsed again with ultra-pure water and treated with pure argon gas for drying. The clean gold electrode was called as bare electrode and it mentioned as Au in the study. The clean

electrode was immersed to 20 mM 6-MCH solution prepared in pure ethanol for 16 h. At the end of this period, the electrode surface was rinsed with pure ethanol to remove 6-MCH molecules that are covalently unattached, and slowly dried with the pure argon.

Covalent binding of Anti-Ocn on 6-MCH modified electrodes

For Anti-Ocn immobilization, 1,4-butanediol diglycidyl ether (1,4-BDE),[26] which is bisoxiranes and contain two epoxy functional groups, was used to activate the hydroxyl groups of 6-MCH molecules on SAM surface under mild conditions. 1,4-BDE solution (7%) was dispersed onto the 6-MCH modified electrode surface and then kept in a dark environment for 1 h. Then, the gold electrodes are gently washed with ultrapure water and then dried again with a stream of pure argon (Au/6-MCH/1,4-BDE). The electrode surface modified with hydroxyl groups of 6-MCH is capable of forming strong covalent bonds with free reactive epoxy groups of 1,4-BDE. The other end of the bisoxiranes can give reaction with primary amine, hydroxyl, and sulfhydryl groups of compounds.

For this purpose, in the next step, ethanolamine was used as hydroxyl containing ligand. Ethanolamine solution (0.5 M) was spread over the electrode surface and then left for 1 h. Ethanolamine is a heterobifunctional cross-linker and its hydroxyl groups reacts with the other epoxy ends of epoxy-activated Au electrode (Au/6-MCH-1,4-BDE), resulting in a stable, uncharged ether linkage at pH 7.0. 1,4-BDE-activated electrode formed stable covalent bonds to the ethanolamine solution (0.5 M) for 1 h while introducing a hydrophilic spacer arm between the modified electrode surface and the ligand (Au/6-MCH-1,4-BDE/EA). After then, GLT was used to activate the amino terminus of ethanolamine (Au/6-MCH-1,4-BDE/EA/GLT). GLT solution (2.5%) was dropped to the electrode surface and left for 15 min. The electrode was gently washed and then dried again with a stream of pure argon. GLT is the most popular bis-aldehyde homo-bifunctional crosslinking agent used in the immobilizations of biomolecules. When GLT was used as a cross-linking reagent, the reaction between amine groups of EA and Anti-Ocn was considered to proceed through the formation of Schiff bases, a sub-class of imines. By thinking the other crosslinking reactions may also occur, to prevent this GLT was applied to modified Au electrode surface (Au/6-MCH-1,4-BDE/EA) using the two-step procedure. The electrode surface was first activated with GLT for 15 min and after, all excess of GLT on modified electrode surface was washed to prevent the other protein-protein cross-linking reactions. As the last step, 5 µL of Anti-Ocn aliquot (5 ng μL^{-1}) was applied to the electrode surface and incubated for 1 h, (Au/6-MCH-1,4-BDE/EA/GLT/Anti-Ocn). Finally, the electrode surface was washed with distilled water to remove the unattached Anti-Ocn molecules and dried again with pure argon. At the end of this step, Ocn biosensor construction was completed (Figure 1).

Electrochemical measurements and principals

Following each immobilization step, electrochemical analyses including cyclic voltammetry (CV) and EIS were performed to observe the changes in electrode surface and determine Ocn amount in sample. CV was especially used to characterize SAM formation on bare electrode and the surface modifications during Anti-Ocn immobilization to Au electrode surface. 5 mM $K_3[Fe(CN)_6/K_4[Fe(CN)_6]$ solution (1:1) containing 0.1 M KCl was used as redox probe in both electrochemical measurements. This redox probe solution enables easy electron transport over the electroactive species on the electrode surface.[27] Cyclic voltammograms were obtained at potential ranged from −0.1 and 0.5 V, step size: 1 mV, scanning speed: 50 mV/s. EIS were collected in the frequency range between 50.000 and 0.05 Hz at 10 mV of alternating current within redox probe solution.

EIS was used to determine the amount of redox probes associated with changes in the electron transfer resistance (R_{ct}) at Anti-Ocn biosensor surface. The response of fabricated Ocn biosensor were measured for Ocn concentrations varied at the ranged of 10–60 pg μL^{-1}, and the obtained R_{ct}s values for each of measurement related with Ocn concentrations were calculated via the Gamry potentiostate ECM Analyst software. For this purpose, The EIS data obtained under above conditions were analyzed by fitting to the Nyquist plots via software. To prepare the standard calibration curve for Ocn, R_{ct} changes for different Ocn concentrations were calculated using the following equation:

$$\Delta R_{ct} = R_{ct(AntiOcn/Ocn)} - R_{ct(AntiOcn)},$$

where $R_{ct(AntiOcn/Ocn)}$ and $R_{ct(AntiOcn)}$ were defined as the R_{ct} value after Ocn is attached to Anti-Ocn and the R_{ct} value after Anti-Ocn is immobilized on the electrode surface, respectively.

Results and discussion

Anti-osteocalcin immobilization and optimization

After each step of Ocn-biosensor immobilization, the layer formation was characterized using EIS and CV. EIS is sensitive to changes in the surface and a powerful method used for analyzing the complex electrical resistance of a system. It is particularly suitable for detecting binding phenomena on the surface of the physical component in the biosensor area; therefore, it is a valuable and progressive technique.[28] Also, CV technique is used to observe layer by layer immobilization on electrode surface. In this study, the cyclic voltammograms and EIS spectra of each immobilization step of the Anti-Ocn are shown in Figure 2a,b. When the electrode was coated with 6-MCH self-binding monolayer, a sharp increase in the peak current was observed because the hydroxyl groups of 6-MCH probably inhibit the negatively charged ferricyanide against the electrode surface. As shown in Figure 1, after the modification of the electrode surface with 6-MCH, it was observed that the characteristic CV peaks of the electrode were not dielectric.

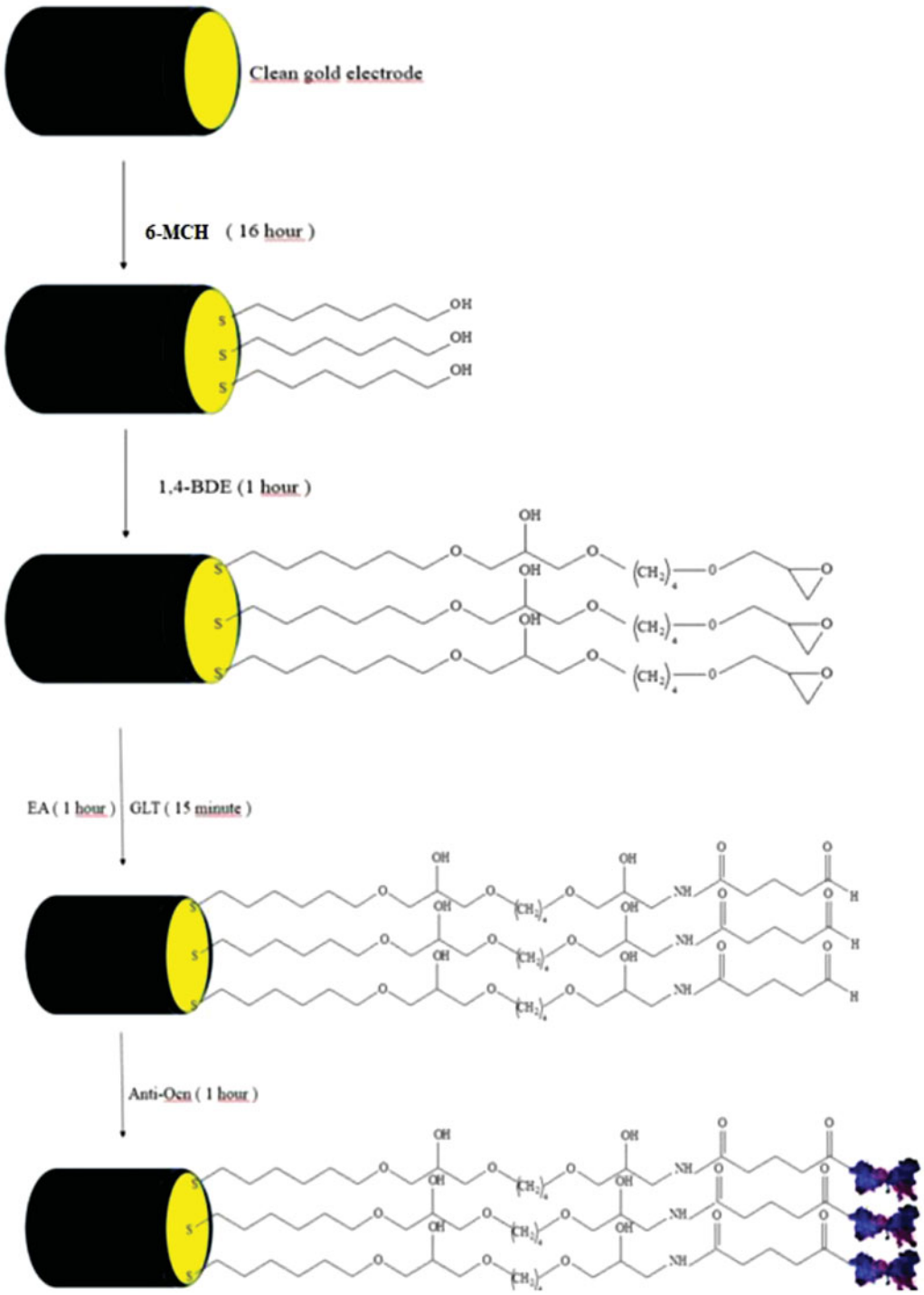

Figure 1. Immobilization steps of the Osteocalcin biosensor.

The immobilization steps of the biosensor were investigated for the effects of 6-MCH concentration, 1,4-BDE concentration, EA concentration, GLT concentration, and Anti-Ocn concentration.

The optimum concentration of 6-MCH to form stable and self-assembled monolayers (SAM) on the electrode surface was determined. For this purpose, Ocn biosensors were fabricated using 6-MCH solutions at concentrations of 10 mM, 20 mM, 30 mM, and 40 mM. R_{ct} values were calculated from Nyquist plots of EIS spectra obtained from Ocn concentrations ranging from 10 to 60 ng μL^{-1}. The calibration graphs were plotted between R_{ct} values versus Ocn concentrations to determine the effect on biosensor response of 6-MCH concentration (Figure 3).

As shown in Figure 3, the biosensor performance was affected by the changes in 6-MCH concentration. An increase in R_{ct} values was seen with the increase of 6-MCH concentration. At high 6-MCH concentrations, R_{ct} values increased because increasing surface density probably blocked the electron transfer at the electrode surface. The highest equation coefficient (R^2) values were calculated as 0.9864 and 0.9857 from the calibration graph prepared for

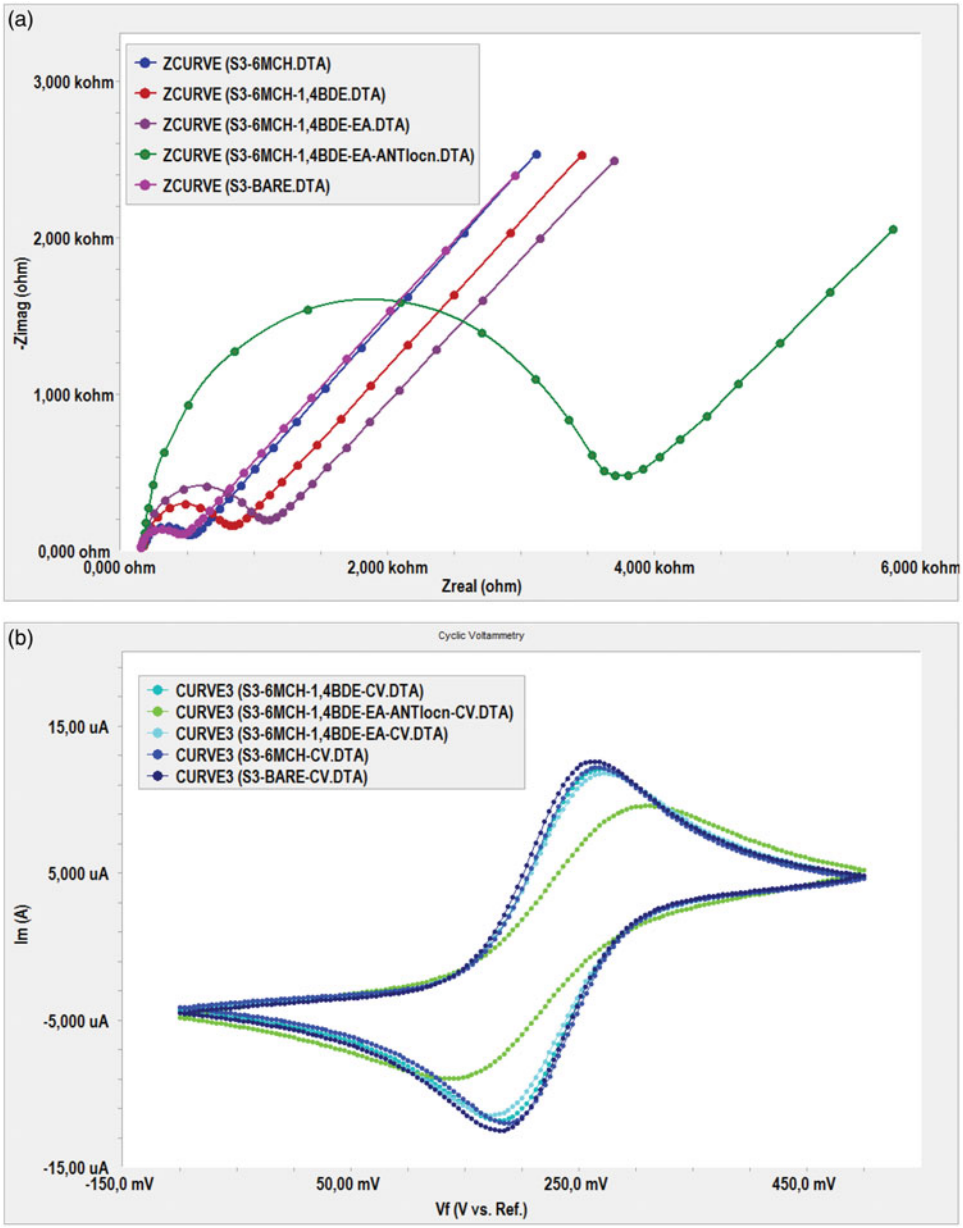

Figure 2. (a) Electrochemical impedance spectra of Anti-Ocn immobilization steps. (b) Cyclic voltammograms of Anti-Ocn immobilization by covalent attachment.

40 mM and 20 mM 6-MCH, respectively. Although the highest R^2 value was found at the concentration of 40 mM 6-MCH, the best biosensor response was determined as 20 mM 6-MCH. It can be said from EIS results that SAM prepared using 20 mM 6-MCH showed minimum blocking effect. Ocn biosensor fabrications were carried out using 20 mM 6-MCH when forming SAM on Au electrode surface in further studies.

The second step in the optimization studies was to determine the effect of 1,4-BDE concentration on biosensor response. For this purpose, the solutions prepared at the different concentrations of 1,4-BDE such as 1%, 4%, 7%, and 10% were used for the construction of biosensors. As seen in Figure 4, R^2 values were determined as 0.9248, 0.9634, 0.9880, and 0.9616, respectively. Both highest R^2 value and the best linearity were found to be at the concentration of 7% 1,4-BDE. According to EIS results, it can be said that the concentration of 7% 1,4-BDE further increased minimum blocking effect caused by 6-MCH.

To investigate the effect of ethanolamine concentration on biosensor responce, Ocn biosensors were prepared using different ethanolamine solutions (0.1 M, 0.5 M, 1 M, and 2 M) and EIS measurements carried out at different Ocn concentrations ranging from 10 to 60 ng μL^{-1}. R^2 values were calculated as 0.8473, 0.9844, 0.9779, and 0.7625, respectively (Figure 5). At higher ethanolamine concentrations (1 M and 2 M) the R_{ct} values were higher, but the ethanolamine solutions prepared at these concentrations solidified with white-opaque appearance on the surface of the working electrode. The difficulty in cleaning excess EA from electrode surface was encountered during the washing process and some deterioration of the biosensor surface was observed due to the detachment of the immobilized molecules on the surface since washing process takes a long time.

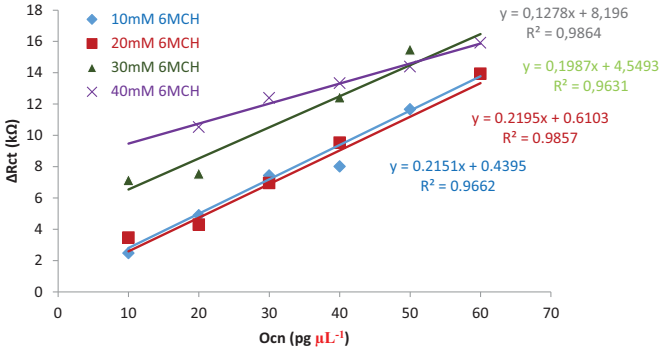

Figure 3. Effect of 6-MCH concentration on biosensor response.

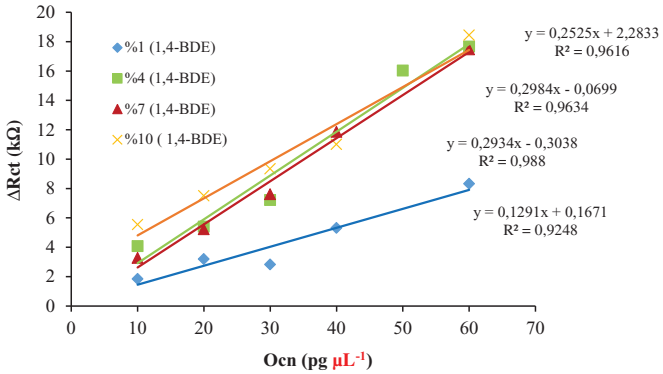

Figure 4. The effect of 1,4-butanediol dithlyceridyl ether concentration on the biosensor response.

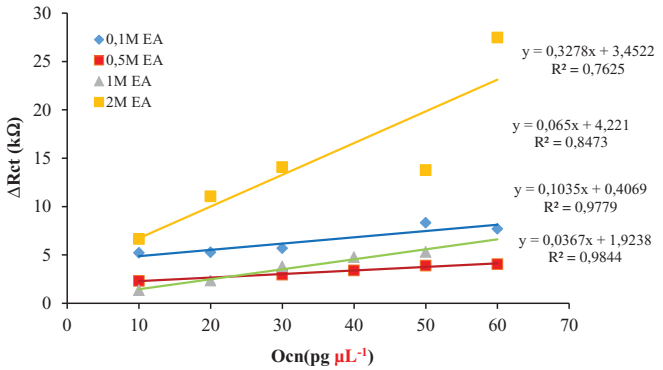

Figure 5. Effect of ethanol concentration on biosensor response.

Therefore, the lower concentration of ethanolamine was chosen for biosensor construction. Optimum ethanolamine concentration was determined as 0.5 M, which had highest R^2 value, though biosensor response was lower.

The next step in the optimization studies was the determination of Anti-Ocn concentration required for effective binding of Ocn. Biosensors were prepared at the different Anti-Ocn concentrations (5 ng μL^{-1}, 10 ng μL^{-1}, 20 ng μL^{-1}, and 30 ng μL^{-1}). As shown in Figure 6, R^2 values were calculated as 0.9948, 0.9787, 0.9925, and 0.9862, respectively. The obtained R_{ct} values showed that the biosensor performance was dependent on the concentration of Anti-Ocn used for the immobilization. The highest R^2 values were calculated as 0.9948 and 0.9925 for 5 ng μL^{-1} and 20 ng μL^{-1} Anti-Ocn, respectively. The highest R^2 value was

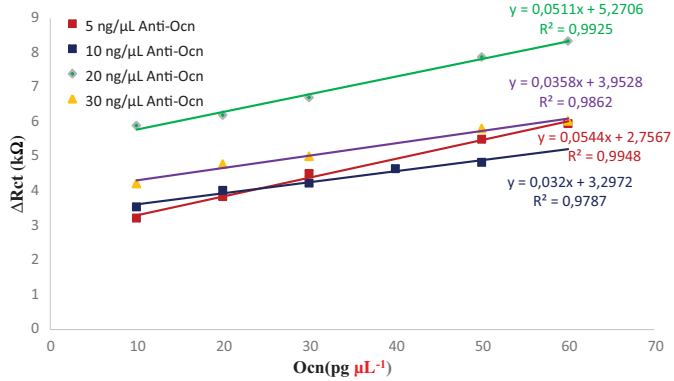

Figure 6. The effect of Anti-Ocn concentration on the biosensor response.

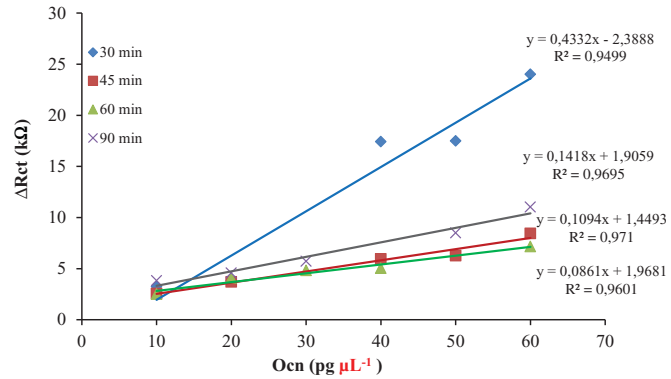

Figure 7. Effect of Ocn incubation time on biosensor response.

relatively found at the concentration of 20 ng μL^{-1} Anti-Ocn. But, when the price of the Anti-Ocn molecule and accordingly the cost of the biosensor fabrication is considered, the optimum Ocn concentration was chosen as 5 ng μL^{-1} instead of 20 ng μL^{-1}.

The interaction of the antibody and antigen influences the binding efficiency and the resistance of the bond in immobilization. Therefore, after determining the most suitable concentrations of all molecules in the immobilization steps, Ocn incubation was performed for 30 min, 45 min, 60 min, and 90 min. As seen in Figure 7, the best biosensor response was determined when Ocn incubated for 45 min.

In addition, the Laviron equation can be used to estimate the concentration of the electroactive protein at the working electrode surface.[29,30] The Laviron equation: $Q = n \times F \times A \times \Gamma$; where Q is the charge, n is the slope of the graphs plotted versus the currents determined from CVs obtained at 10 different scan rate, F is the constant of Faraday, and Γ is the amount of electroactive molecule on the electrode surface.[31] For this purpose, CVs were obtained at 10 different scan rate from 10 mVs^{-1} to 100 mVs^{-1} in the potential range of −0.1, 0.5 V for Au-Bare electrode and Au/6-MCH/1,4-BDE/EA/GLT/Anti-Ocn electrode, and the Γ values were calculated as 1.9 10^{-7} mol/cm^2 and 2.9 10^{-7} mol/cm^2, respectively. The Γ values of Au/6-MCH/1,4-BDE/EA/GLT/Anti-Ocn electrode is distinctly higher than obtained for bare electrode, indicating that the immobilization of Anti-Ocn was success.

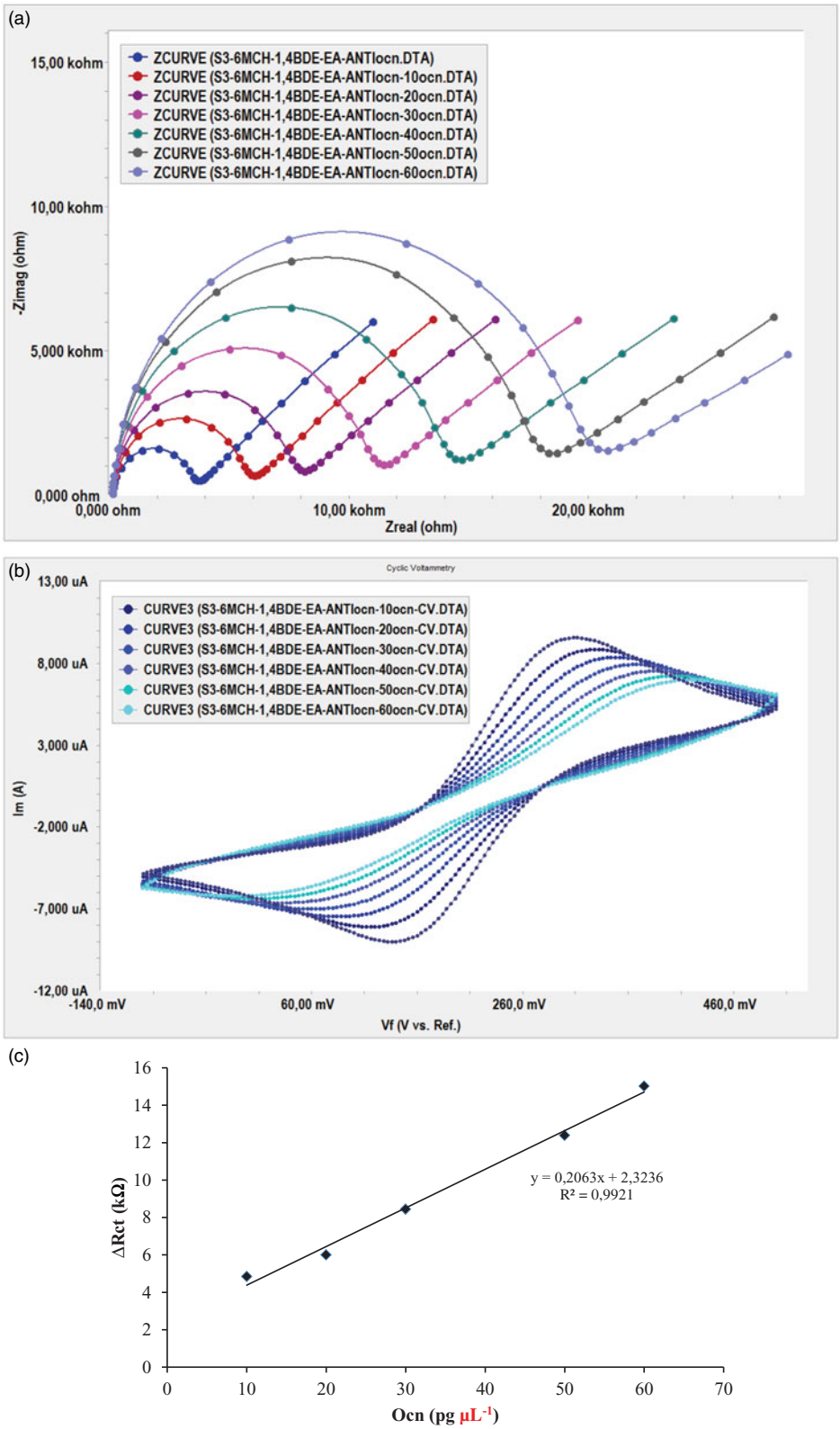

Figure 8. (a) Nyquist curves obtained in the Ocn concentration range of 10–60 pg μL^{-1}. (b) Cyclic voltamograms obtained using Ocn biosensor in the ranged of 10–60 pg μL^{-1} Ocn concentration. (c) The calibration graph of Ocn biosensor in the range of 10–60 pg μL^{-1}.

Analytical characteristics of the biosensor

In order to determine the linear determination range with Ocn biosensor prepared in the optimized immobilization conditions [6-MCH (20 mM), 1,4-BDE (7%), GLT (2.5%), Anti-Ocn (10 ng μL^{-1}), and Ocn (5 pg μL^{-1}) 45 min], the studies on the quantitative determination of Ocn were performed in the range of 10–60 pg μL^{-1} Ocn concentration. Nyquist curves and CV plots obtained for different Ocn concentrations are given in Figure 8a,b.

The semi-circle diameter of Nyquist curves increased linearly with increasing Ocn concentrations. The increase in

Table 1. Comparison of osteocalcin biosensor studies.

Features	This study	Min-Ho Lee et al.	Patricia Khashayar et al.
Method	Electrochemical ımpedance spectroscopy (EIS)	Amperometry	Differential pulse voltammetry (DPV)
Electrode type	Gold (Au) electrode	Gold (Au) electrode	Gold (Au) electrode
Detection limit	10–60 pg μL^{-1}	1–100 ng mL^{-1}	2.5–90 ng mL^{-1}
LOD	1.1 pg μL^{-1}	N.R	0.65 ng mL^{-1}
LOQ	3.7 pg μL^{-1}	N.R	1.97 ng mL^{-1}

Table 2. Reproducibility of the Ocn biosensor in the range of 10–60 pg μL^{-1} Ocn concentration.

Biosensor number	Linearity coefficient (R^2)	Equation of a line	Linear range (pg μL^{-1})
1	0.992	$y = 0.206x + 2.324$	10–60
2	0.992	$y = 0.091x + 0.775$	10–60
3	0.987	$y = 0.108x + 1.343$	10–60
4	0.987	$y = 0.201x - 0.234$	10–60
5	0.986	$y = 0.299x - 0.037$	10–60
6	0.9869	$y = 0.3311x - 1.662$	10–60
7	0.980	$y = 0.247x + 2.143$	10–60
8	0.978	$y = 0.485x - 1.092$	10–60

Table 3. The results of the Ocn measurement using proposed biosensor in artificial serum samples.

Ocn level in artificial serum (pg μL^{-1})	Measured Ocn (pg μL^{-1}) level	Recovery (%)
10	9.85	98.5
20	20.93	104.6
30	28.82	96.06
50	50.54	101.08
60	59.85	99.75

the Ocn concentration increased the charge transfer resistance when analyzed in the linear range of 10–60 pg μL^{-1} as the detection range for Ocn measurements. Ocn levels in serum changes between 9 and 42 pg μL^{-1}. The obtained results showed that Anti-Ocn biosensor precisely determined Ocn concentration.

According to the obtained results, the fabricated Anti-Ocn biosensor permits the specific determination of the Ocn molecule. The standard calibration graph for Ocn is shown in Figure 8c, which was plotted with respect to the changes in R_{ct} after Ocn addition to electrode surface.

Clinically, Ocn is determined by ELISA and RIA methods. In the literature, there are a few biosensor studies for Ocn determination. Khashayar et al. developed a biosensor based on Differential Pulse Voltametry (DPV) for Ocn determination. All immobilization steps of the biosensor were controlled by EIS. The designed biosensor measured Ocn concentrations by immobilizing L-Glutathione Reduced (GSH), EDC (1-Ethyl-3-(3-dimethylaminopropyl)-carbodiimide) N-hydroxysulfoxuccinimide (sulfo-NHS), Anti-Ocn onto the gold electrode surface, respectively.[32] The same group reported the another article and characterized the immobilization steps used in fabrication of this Ocn biosensor.[33]

Min-Ho Lee et al. designed an amperometric biosensor. The biosensor construction was started by immersing in dimethyl sulfoxide (DMSO) solution containing dithiobis-N-succinimidyl propionate (DTSP). After rinsing with acetone, and conditioning in phosphate buffer solution (PBS) of the electrode, the biosensor fabrication was completed applying horseradish peroxidase (HRP) conjugated antibody (Anti-Ocn) to the electrode surface. The amperometric measurements were done for each step of biosensor fabrication.[34] The presented biosensor was compared with these Ocn biosensors in Table 1.

In order to determine the reproducibility of the Ocn biosensor, eight different biosensors were prepared under optimum immobilization conditions [6-MCH (20 mM), 1,4-BDE (7%), GLT (2.5%), Anti-Ocn (10 ng μL^{-1}), and Ocn (5 pg μL^{-1}) 45 min] and measurements in the concentration range of 10–60 pg μL^{-1} were carried out. The results showed that the biosensor developed here can be used reproducibly for Ocn detection and measurement. The results can be seen in Table 2.

Also, limit of detection (LOD) and limit of quantification (LOQ) values were calculated according to the IUPAC recommendations, as 1.1 pg μL^{-1} and 3.7 pg μL^{-1}, respectively.[35] These results showed that the developed biosensor has high sensitivity for the detection and quantification of Ocn.

In addition, the developed Ocn biosensor was applied to artificial serum samples. With artificial serum samples, it was investigated whether antigen-antibody interactions is affected by salts in serum. All dilutions for the Ocn were carried out with artificial serum solution. The effect of the artificial serum on the biosensor response was examined in the linear determination range. Measurements were carried out in artificial serum with biosensors prepared under optimum immobilization conditions. The results were given in Table 3.

The experiments in the artificial serum samples demonstrates that the salts and other biomolecules in the artificial serum have no effect on the biosensor response. The biosensor developed for this reason has the potential for a precise and specific determination of Ocn in real serum samples.

Conclusions

As a result, a new, inexpensive, fast, high-precision, and highly repeatable biosensor was developed using 1,4-BDE as the immobilization material onto SAM for the first time in the literature for the determination of Ocn. This fabricated biosensor may be an alternative for determination of Ocn to high-cost techniques such as ELISA and RIA. In addition, it was determined that the biomolecules and salts in the artificial serum did not affect the Ocn measurement results. In this regard, it is possible to use the proposed Ocn-biosensor safely for Ocn determination.

Funding

This study is supported by Trakya University Scientific Research Foundation (Project Number: TUBAP-2016/106).

References

[1] Kanis, J.A.; Kanis, J.A. Assessment of Fracture Risk and Its Application to Screening for Postmenopausal Osteoporosis: Synopsis of a WHO Report. WHO Study Group. *Osteoporosis Int.* **1994**, *4*, 368–381. DOI: 10.1007/BF01622200.

[2] Lee, S.W.; Jo, H.H.; Kim, M.R.; Kim, J.H.; You, Y.O. Association between Osteocalcin and Metabolic Syndrome in Postmenopausal Women. *Arch. Gynecol. Obstet.* **2015**, *292*, 673–681. DOI: 10.1007/s00404-015-3656-7.

[3] Edwards, M.H.; Dennison, E.M.; Aihie Sayer, A.; Fielding, R.; Cooper, C. Osteoporosis and Sarcopenia in Older Age. *Bone* **2015**, *80*, 126–130. DOI: 10.1016/j.bone.2015.04.016.

[4] Khashayar, P.; Meybodi, H.R.A.; Homami, M.R.; Heshmat, R.; Larijani, B. The Prevalence of Osteoporosis in an Iranian Population. *J. Clin. Densitometry* **2010**, *13*, 1–112. DOI: 10.1016/j.jocd.2010.01.022.

[5] Oden, A.; McCloskey, E.V.; Kanis, J.N.; Harvey, N.C.; Johansson, H. Burden of High Fracture Probability Worldwide: Secular Increases 2010–2040. *Osteoporos. Int.* **2015**, *26*, 2243–2248. DOI: 10.1007/s00198-015-3154-6.

[6] Liu, L.; Webster, T.J. In Situ Sensor Advancements for Osteoporosis Prevention, Diagnosis, and Treatment. *Curr. Osteoporos. Rep.* **2016**, *14*, 386–395. DOI: 10.1007/s11914-016-0339-7.

[7] Pagani, F.; Francucci, C.M.; Moro, L. Markers of Bone Turnover: Biochemical and Clinical Perspectives. *J. Endocrinol Invest* **2005**, *28*, 8–13.

[8] Parmar, B.J.; Longsine, W.; Sabonghy, E.P.; Han, A.; Tasciotti, E.; Weiner, B.K.; Righetti, R. Characterization of Controlled Bone Defects Using 2D and 3D Ultrasound Imaging Techniques. *Phys Med Biol* **2010**, *55*, 16.

[9] Seibel, M.J.; Robins, S.P.; Bilezikian, J.P. *Dynamics of Bone and Cartilage Metabolism: Principles and Clinical Applications*. Academic Press, London, **2006**.

[10] Seibel, M.J. Biochemical Markers of Bone Turnover: Part I: Biochemistry and Variability. *Clin. Biochem. Rev.* **2005**, *26*, 97–122.

[11] Morris, H.A.; Eastell, R.; Jorgensen, N.R.; Cavalier, E.; Vasikaran, S.; Chubb, S.A.P.; Kanis, J.A.; Cooper, C.; Makris, K. Clinical Usefulness of Bone Turnover Marker Concentrations in Osteoporosis. *Clin. Chim. Acta* **2017**, *467*, 34–41. DOI: 10.1016/j.cca.2016.06.036.

[12] Reginster, J.-Y.; Collette, J.; Neuprez, A.; Zegels, B.; Deroisy, R.; Bruyere, O. Role of Biochemical Markers of Bone Turnover as Prognostic Indicator of Successful Osteoporosis Therapy. *Bone* **2008**, *42*, 832–836. DOI: 10.1016/j.bone.2008.01.021.

[13] Hauschka, P.V.; Lian, J.B.; Cole, D.E.; Gundberg, C.M. Osteocalcin and Matrix Gla Protein: Vitamin K-Dependent Proteins in Bone. *Physiol. Rev.* **1989**, *69*, 990–1047. DOI: 10.1152/physrev.1989.69.3.990.

[14] Hoang, Q.Q.; Sicheri, F.; Howard, A.J.; Yang, D.S.C. Bone Recognition Mechanism of Porcine Osteocalcin from Crystal Structure. *Nature* **2003**, *425*, 977–980. DOI: 10.1038/nature02079.

[15] Lombardi, G.; Perego, S.; Luzi, L.; Banfi, G. A Four-Season Molecule: Osteocalcin. Updates in Its Physiological Roles. *Endocrine* **2015**, *48*, 394–404. DOI: 10.1007/s12020-014-0401-0.

[16] Nimptsch, K.; Hailer, S.; Rohrmann, S.; Gedrich, K.; Wolfram, G.; Linseisen, J. Determinants and Correlates of Serum Undercarboxylated Osteocalcin. Ann. *Nutr. Metab.* **2008**, *51*, 6563–6570.

[17] Power, M.J.; Fottrell, P.F. Osteocalcin: Diagnostic Methods and Clinical Applications. *Crit. Rev. Clin. Lab. Sci.* **1991**, *28*, 287–335. DOI: 10.3109/10408369109106867.

[18] Delmas, P.D. Biochemical markers of bone remodeling. In: Papapoulos, Ed. *Osteoporosis*. Elsevier Science, Amsterdam, **1996**; pp. 191–204.

[19] Jagtap, V.R.; Ganu, J.V.; Nagane, N.S. BMD and Serum Intact Osteocalcin in Postmenopausal Osteoporosis Women. *Ind. J. Clin. Biochem.* **2011**, *26*, 70–73. DOI: 10.1007/s12291-010-0074-2.

[20] Barton, A.C.; Davis, F.; Higson, S.P.J. Labeless Immunosensor Assay for the Stroke Marker Protein Neuron Specific Enolase Based upon an Alternating Current Impedance Protocol. *Anal. Chem.* **2008**, *80*, 9411–9416. DOI: 10.1021/ac801394d.

[21] Ahlqvist, E.; Osmark, P.; Kuulasmaa, T.; Pilgaard, K.; Omar, B.; Brøns, C.; Kotova, O.; Zetterqvist, A.V.; Stancáková, A.; Jonsson, A.; et.al. A Link between GIP and Osteopontin in Adipose Tissue and Insulin Resistance. *Diabetes* **2013**, *62*, 2088–2094. DOI: 10.2337/db12-0976.

[22] Berezin, A.E.; Kremzer, A.A. Circulating Osteopontin as a Marker of Early Coronary Vascular Calcifcation in Type Two Diabetes Mellitus Patients with Known Asymptomatic Coronary Artery Disease. *Atherosclerosis* **2013**, *229*, 475–481. DOI: 10.1016/j.atherosclerosis.2013.06.003.

[23] Sekenis, T.; Garifallou, G.; Davis, G.Z.; Millner, F.; Pinacho, P.A.; D, G.; Sanchez-Baeza, F.; Marco, M.P.; Gibson, T.D.; Higson, S.P. Detection of Fluoroquinolone Antibiotics in Milk via a Labeless Immunoassay Based upon an Alternating Current Impedance Protocol. *Anal. Chem.* **2008**, *80*, 9233–9239. DOI: 10.1021/ac8014752.

[24] Aydin, M.; Aydin, E.B.; Sezginturk, M.K. A Highly Selective Electrochemical Immunosensor Based on Conductive Carbon Black and Star PGMA Polymer Composite Material for IL-8 Biomarker Detection in Human Serum and Saliva, *Biosens. Bioelectron* **2018**, *117*, 720–728.

[25] Lucarelli, F.; Marrazza, G.; Turner, A.P.F.; Mascin, M. Carbon and Gold Electrodes as Electrochemical Transducers for DNA Hybridisation Sensors. *Biosens. Bioelectron.* **2004**, *19*, 515–530. DOI: 10.1016/S0956-5663(03)00256-2.

[26] Piperno, S.; Bui, B.T.S.; Haupt, K.; Gheber, L.A. Immobilization of Molecularly Imprinted Polymer Nanoparticles in Electrospun Poly (Vinylalcohol) Nanofibers. *Langmuir* **2011**, *27*, 1547–1550. DOI: 10.1021/la1041234.

[27] Ozcan, B.; Sezginturk, M.K. A Novel Label Free Immunosensor Based on Single-Use ITO-PET Electrodes for Detection MAGE1 Protein. *J. Electroanal. Chem.* **2017**, *792*, 31–38.

[28] Gutes, A.; Cespedes, F.; Alegret, S.; Del Valle, M. Determination of Phenolic Compounds by a Polyphenol Oxidase Amperometric Biosensor and Artificial Neural Network Analysis. *Biosens. Bioelectron.* **2005**, *20*, 1668–1673. DOI: 10.1016/j.bios.2004.07.026.

[29] Lanzellotto, C.; Favero, G.; Antonelli, M.L.; Tortolini, C.; Cannistraro, S.; Coppari, E.; Mazzei, F. Nanostructured Enzymatic Biosensor Based on Fullerene and Gold Nanoparticles: Preparation, Characterization and Analytical Applications. *Biosens. Bioelectron.* **2014**, *55*, 430–437. DOI: 10.1016/j.bios.2013.12.028.

[30] Yagati, A.K.; Lee, T.; Min, J.; Choi, J.-W. An Enzymatic Biosensor for Hydrogen Peroxide Based on CeO_2 Nanostructure Electrodeposited on ITO Surface. *Biosens. Bioelectron.* **2013**, *47*, 385–390. DOI: 10.1016/j.bios.2013.03.035.

[31] Laviron, E. General Expression of the Linear Potential Sweep Voltammogram in the Case of Diffusionless Electrochemical Systems. *J. Electroanal. Chem.* **1979**, *101*, 19–28. DOI: 10.1016/0368-1874(79)87084-7.

[32] Khashayar, P.; Amoabediny, G.; Hosseini, M.; Verplancke, R.; Razi, F.; Vanfleteren, J.; Larijani, B. An Electrochemical Biosensor Based on AuNP-Modified Gold Electrodes for Selective Determination of Serum Levels of Osteocalcin. *IEEE*

Sensors J. **2017**, *17*, 3367–3374. DOI: 10.1109/JSEN.2017.2684903.

[33] Khashayar, P.; Amoabediny, G.; Larijani, B.; Hosseini, M.; Vanfleteren, J. Fabrication and Verification of Conjugated AuNP-Antibody Nanoprobe for Sensitivity Improvement in Electrochemical Biosensors. *Sci. Rep.* **2017**, *7*, 16070.

[34] Lee, M.H.; Kim, H.Y.; Seo, Y.T.; Lee, K.N. Simple, Fast, and Quantitative Detection of Affinity Reaction of Osteocalcin Using Amperometric Method. *IEEE* **2014**, *2*, 772–775.

[35] McNaught, A.D.; Wilkinson, A. *Compendium of Chemical Terminology*. Blackwell Science, Oxford, **1997**, ISBN 0865426848